Tunneling, Zero-Bias Anomalies, and Small Superconductors

H. R. Zeller and I. Giaever

General Electric Research and Development Center, Schenectady, New York 12301

(Received 30 December 1968)

We have prepared tunnel junctions which contain small Sn particles imbedded in the oxide barrier. The size distribution of the small particles has been determined from electron micrographs. The electrical characteristics of these junctions were measured in the temperature range 1–300°K and in magnetic fields up to 100 kOe. All junctions show a large temperature-dependent resistance peak at zero bias and at low temperatures. The resistance peak increases in magnitude when the Sn particles are made superconducting. A simple model based upon the capacitance of the particles can account quantitatively for this behavior. We believe that a simple extension of this model can account for at least some of the previously reported zero-bias resistance anomalies. From the experiment, it is also possible to extract information about the superconductivity of small particles. We find that Sn particles down to at least a radius $r \sim 25$ Å are superconducting. The transition temperature of the particles increases with decreasing particle size and reaches 4.2°K for particles with $r \sim 70$ Å, compared with $T_c = 3.7$°K for bulk Sn. In the radius range $r > 100$ Å, the critical field of the particles can be described in terms of a theory by De Gennes and Tinkham. Smaller particles have a much higher critical field, which increases more rapidly with decreasing radius than predicted by that theory.

I. INTRODUCTION

IN the last few years electron tunneling has been used extensively in the study of superconductors.[1] When a metal becomes superconducting, the electron density of states changes and this change is directly reflected in the current-voltage characteristic of a tunnel junction. A tunnel junction is simply a capacitor in which the plates are spaced only a few tens of angstroms apart. Most tunnel junctions are made from evaporated metal films separated by a natural oxide layer grown on the first evaporated film. We have recently[2] extended the method of tunneling to study very small metal particles. The sample now resembles a capacitor with small metal spheres imbedded in the dielectric separating the plates. Again the spacing is so close that electrons can flow from one capacitor plate to the other by tunneling; however, most of the electrons flow via the small metal particles imbedded in the dielectric. By using particles of a superconducting metal we are able to study the size dependence of the superconducting properties, because again the superconducting density of state is reflected in the current-voltage characteristic. Previously, the superconductivity of small particles has been studied by magnetic susceptibility[3] and by Knight-shift measurements.[4]

Since the particles are electrically insulated from each other and charge flow between the particles and the electrodes is only by tunneling, the electronic properties of the particles are to a good approximation those of a free particle. The deviations in some of the physical properties of a small particle from bulk matter have been discussed by, among others, Fröhlich[5] and Kubo.[6]

One of the most important reasons for deviations is that the spacing of the electron energy levels in a small particle cannot be assumed to be small compared to other relevant energies, such as the thermal energy, the electron or nuclear spin Zeeman energy, the superconducting energy gap, and so on. The reason for this energy spacing is that the electron wave functions have to satisfy the boundary conditions imposed by the small particle. For a particle with an arbitrary shape, the electron levels are assumed to be essentially nondegenerate and the splitting is, therefore, of the order ξ/N, where ξ is the Fermi energy and N the number of conduction electrons. For a Sn particle with a radius $r \sim 50$ Å the spacing is of the order 0.1 meV or 1°K in units of kT.

Several authors have predicted a lower size limit for the occurrence of superconductivity. Anderson[7] predicted that superconductivity should disappear when the spacing of the electronic levels in the particle becomes comparable to the superconducting energy gap. Using the bulk energy gap results in a critical radius of about 25 Å for Sn; for smaller particles superconductivity is not possible. Markowitz[8] has added a Coulomb term to the conventional BCS Hamiltonian.[9] Two neighboring regions in a superconductor have the maximum correlation energy when they have the same phase. However, this would produce an uncertainty in the number of electrons in each region and implies large charge fluctuations. Since the superconductor cannot have both maximum correlation energy and uniform charge density, i.e., minimum Coulomb repulsion energy, it optimizes the two. For a small particle the Coulomb term becomes important and, according to Markowitz, leads to occupied singlet states in the ground state of a small superconductor sphere with a

[1] *Tunneling Phenomena in Solids*, edited by E. Burstein and S. Lundqvist (Plenum Press, New York, 1969).
[2] I. Giaever and H. R. Zeller, Phys. Rev. Letters **20**, 1504 (1968).
[3] D. Shoenberg, Proc. Roy. Soc. (London) **A175**, 49 (1940).
[4] F. Reif, Phys. Rev. **102**, 1417 (1956).
[5] H. Fröhlich, Physica **IV**, 406 (1937).
[6] R. Kubo, J. Phys. Soc. Japan **17**, 975 (1962).

[7] P. W. Anderson, J. Phys. Chem. Solids **11**, 26 (1959).
[8] D. Markowitz, Physics **3**, 199 (1967).
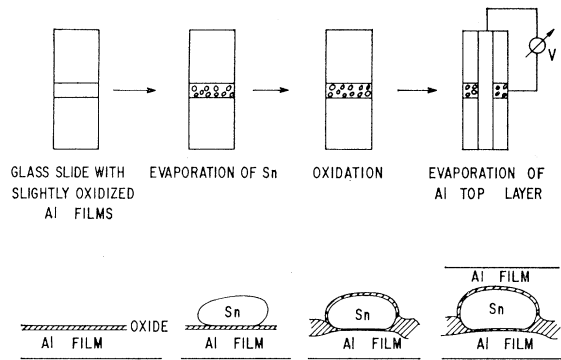[9] J. Bardeen, L. N. Cooper, and J. R. Schrieffer, Phys. Rev. **108**, 1175 (1957).

FIG. 1. Preparation of the tunnel junction containing Sn particles. Because of the faster oxidation of Al with respect to Sn, the oxide in the space between the particles is much thicker than the oxide at the surface of the particles, as sketched schematically in the cross section of the samples.

radius $r < 500$ Å and a destruction of superconductivity around $r \sim 100$ Å. Markowitz's numerical calculations hold for a completely free particle and do not apply directly to our case, since in our experiment the Coulomb interactions are screened to some extent by the matrix in which the particles are imbedded.

All junctions containing metal particles show a large resistance peak at low temperatures and at zero bias even when the particles are in the normal state. Qualitatively, similar behavior has been found by others in impurity-doped junctions; for instance, in Al-I-Ag (I=insulator) junctions doped with chromium, copper, or titanium.[10,11] Shen and Rowell[12] first identified the so-called giant zero-bias resistance peak in Cr-I-Ag junctions, and, in general, the zero-bias anomalies have been thought to be due to scattering of the tunneling electrons by localized magnetic moments in the
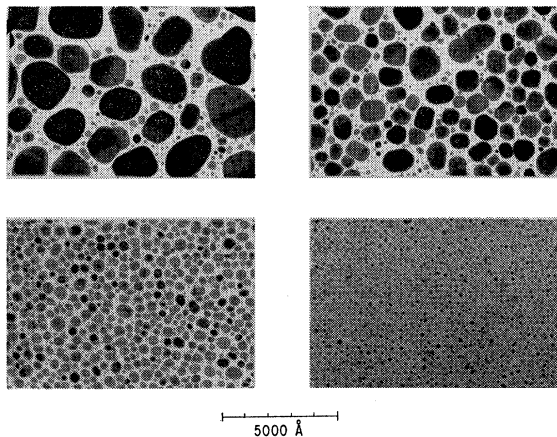

FIG. 2. Electron micrographs of Sn particles on an oxidized Al film for four different samples.

barrier.[13-16] Calculations of the effect by Appelbaum[17] and by Anderson[18] show that the scattering model gives either a peak or dip in the zero-bias resistance depending on the sign of the exchange interaction between the electron and the localized moment. The model seems to explain the small magnetic-field–dependent zero-bias resistance dip observed by several authors,[10,12] but no satisfactory explanation of the giant zero-bias anomaly has emerged. We will show that in the systems which we have investigated the origin of the zero-bias resistance peak can be explained by a simple model and that it is a rather trivial effect.

II. SAMPLE PREPARATION AND EXPERIMENTAL TECHNIQUE

Al-Al$_2$O$_3$-Al junctions containing Sn particles in the oxide have been prepared in the following way: After evaporation of the first Al electrode onto a glass slide, the film was oxidized in air at 100 Torr for approxi-
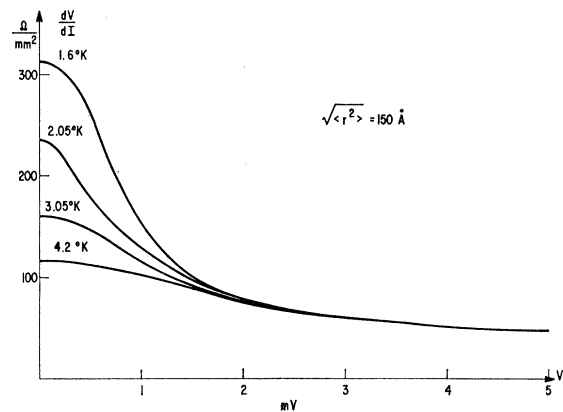

FIG. 3. Dynamical resistance-versus-voltage characteristic for normal particles at different temperatures. The average particle radius is 150 Å. A magnetic field of 35 kOe was applied to keep the particles in the normal state.

mately 1 min. Next, Sn was evaporated onto the slightly oxidized Al film. The amount of Sn evaporated could be controlled using a quartz thickness monitor. The Sn agglomerates into small particles whose average size depends mostly upon the amount of Sn evaporated and the temperature of the substrate. Our substrate was always kept at approximately room temperature. The film was then exposed for 1 h to air at atmospheric pressure. Since Al oxidizes much faster than Sn, the space between the particles is filled with a rather thick Al oxide, while the particles are covered only with a

[10] F. Mezei, Phys. Letters **25A**, 534 (1967).
[11] A. F. G. Wyatt and D. J. Lythall, Phys. Letters **25A**, 541 (1967).
[12] L. Y. L. Shen and J. M. Rowell, Phys. Rev. **165**, 566 (1968).

[13] J. Rowell, in Ref. 1.
[14] J. Appelbaum, J. C. Phillips, and G. Tzouras, Phys. Rev. **160**, 554 (1967).
[15] J. Solyom and A. Zawadowsky, Physik Kondensierten Materie **7**, 325 (1968).
[16] See Ref. 15, p. 342.
[17] J. Appelbaum, Phys. Rev. Letters **17**, 91 (1966); Phys. Rev. **154**, 633 (1967).
[18] P. W. Anderson, Phys. Rev. Letters **17**, 95 (1966).

relatively thin layer of Sn oxide. Finally, the Al counter-electrode was evaporated. Figure 1 shows schematically the junctions prepared in this manner.

At the same time we evaporated Sn onto our sample, we also exposed another Al film about 200 Å thick to the Sn vapor. This Al film had been deposited on rock salt substrate. It is subsequently removed from the substrate in water and used for direct electron micrographs. Electron micrographs of this film enabled us to determine the distribution of particle sizes. In Fig. 2 typical electron micrographs are shown. The distance between the particles is of the order of the particle size for particles with a radius >50 Å and greater for smaller particles. This makes any tunneling between particles completely negligible. The top Al layer essentially fills up the free space between the particles and gives a fairly effective screening of the capacitive interaction between the particles.

The current-versus-voltage and resistance-versus-voltage characteristic of the junctions prepared in this

FIG. 5. Voltage dependence of the dynamical conductance of three difference junctions with different average particle radii. The applied field of 85 kOe is sufficient to keep the particles normal for curves a and b but in curve c a small fraction of the particles is still superconducting.

to plot conductance versus voltage and conductance versus temperature. In Fig. 4 the zero-bias conductance is plotted versus temperature, and, as can be seen, the relationship is linear. In Fig. 5, the conductance versus voltage is shown for three different samples; the conductivity increases linearly with voltage for small voltages and saturates for larger voltages. The voltage where the conductance saturates is strongly dependent on the particle size. For smaller particles the saturation occurs at higher voltages as can also be seen in Fig. 5.

B. Particles in the Superconducting State

So far we have discussed only the properties of the junction when the particles are normal. The particles can be kept normal below the superconducting transition temperature by the application of a large magnetic field. When the particles are switched from the normal to the superconducting state by removing the applied field, the main effect is that the resistance at zero bias
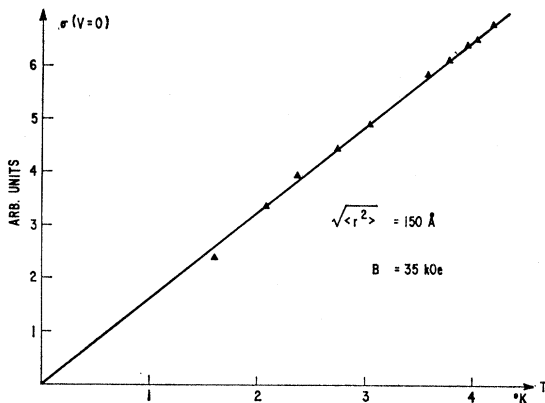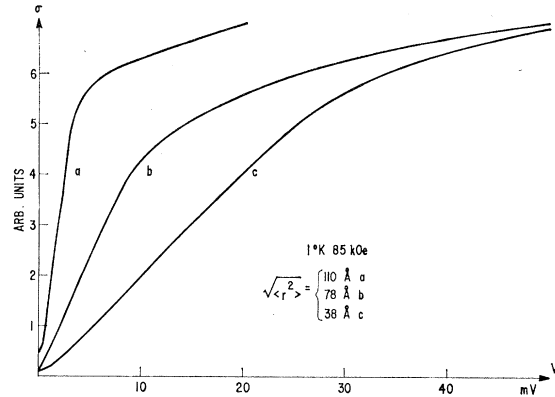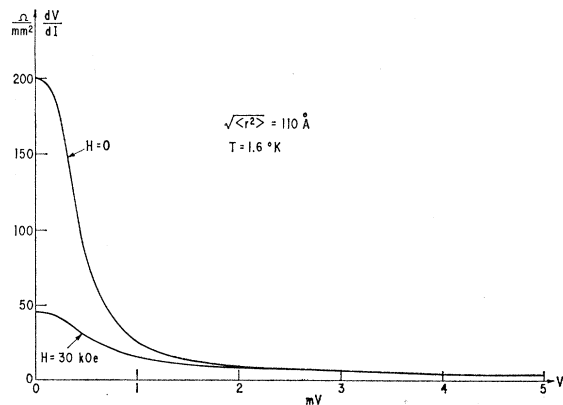

FIG. 4. Temperature dependence of the conduction at zero bias for a junction with average particle radius of 150 Å. A field of 35 kOe was applied to keep the particles in the normal state.

matter have been measured in the temperature range of 1°K–300°K and for magnetic fields up to 100 kOe.

III. EXPERIMENTAL RESULTS

A. Particles in Normal State

All junctions show a resistance maximum at zero bias. The effect may be present at room temperature and increases with decreasing temperature. The half-width of the resistance peak is a few times kT, where k is the Boltzmann constant and T is the temperature in degrees Kelvin. At low temperatures the zero-bias resistance is inversely proportional to the temperature while the resistance at voltages $V \gg kT/e$ is largely temperature-independent, where e is the charge of an electron. A typical resistance-voltage plot is shown in Fig. 3.

Rather than plotting resistance versus voltage, the quantity directly measured in our experiment, we chose

FIG. 6. Dynamical resistance-versus-voltage characteristics for particles in the normal and superconducting state at $T=1.6°$K. As can be seen from Fig. 9 practically all particles are normal at $H=30$ kOe.

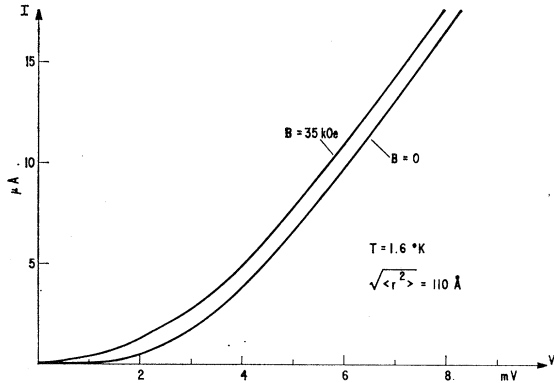Fig. 7. Current-versus-voltage characteristic of a junction with average particle radius $r=110$ Å at 1.6°K for $H=0$ (particles superconducting) and $H=35$ kOe (particles normal).

increases, as shown in Fig. 6. This resistance increase reflects the change in the electron density of states in the particle when it passes from its normal into its superconducting state.

If we look at the current-voltage characteristic of a junction containing large Sn particles, for all practical purposes the characteristic is identical to two separate, conventional $Al-Al_2O_3-Sn$ junctions connected in series; thus, when Sn is superconducting we get a rather sharp current step at a voltage which corresponds to the energy gap (2Δ) of Sn.[19] For smaller particles this step is smeared out. In a conventional metal-insulator-metal tunnel junction the current at a fixed voltage is independent of whether the metal is in the superconducting or the normal state for $eV\gg\Delta$, where Δ is half the energy gap of the superconductor. However, in our experiment the current at a fixed voltage is smaller for the particles being superconducting even when $eV\gg\Delta$
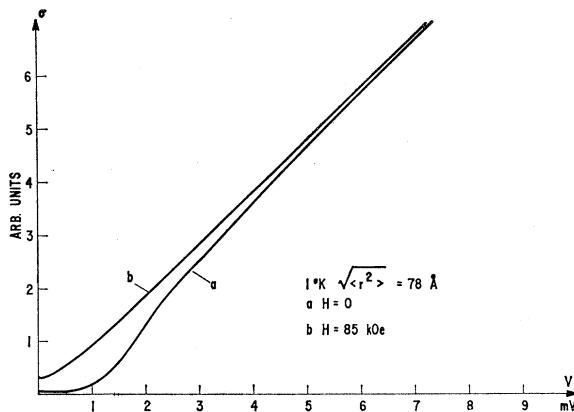

Fig. 8. Voltage dependence of the dynamical conductivity for a junction at $T=1$°K. At $H=0$ the particles are superconducting, at $H=85$ kOe they are normal. Note the similarity between this figure and the *current*-versus-voltage plot of a conventional metal-insulator-metal tunnel junction with one of the metals superconducting.

[19] I. Giaever, H. R. Hart, and K. Megerle, Phys. Rev. 126, 941 (1962).

as illustrated in Fig. 7. A similar shift has been reported by Shen[20] for junctions prepared in a different manner. The maximum observed shift in the voltage for a fixed current is of order Δ/e.

For particles with a radius below $r\sim200$ Å the step due to the peak in the superconducting density of states of the particles appears in the conductivity rather than in the current as for a conventional junction. Figure 8 shows the voltage dependence of the conductivity for the particles in the superconducting and in the normal state. The picture is qualitatively similar to *current* versus voltage for a conventional superconducting tunnel junction.

At voltages $eV\lesssim\Delta$ the conductivity or, as directly measured, the resistance of the junction depend upon a magnetic field. Above the superconducting transition temperature T_c the magnetic field dependence disappears.

Particles with a radius of about 1000 Å show a T_c close to the bulk T_c of Sn. Since the field dependence of

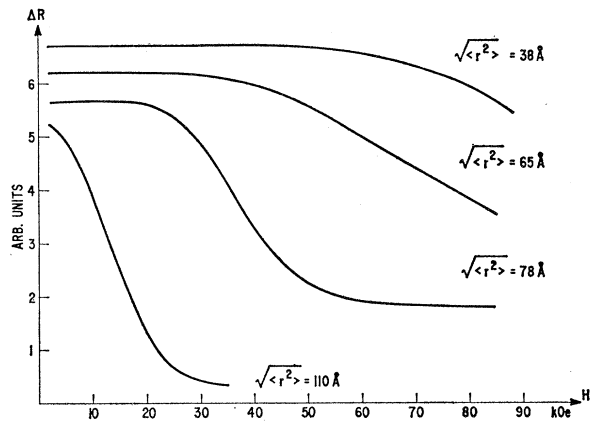Fig. 9. Magnetic field dependence of the junction resistance at zero bias and $T=1$°K. We define the critical field as the field where the resistance drop is half the total drop.

the resistance is small close to the transition temperature and since it is a smoothly varying function of the temperature, it is difficult to determine T_c accurately by this method. However, all junctions containing particles with a radius in the range 25–70 Å showed evidence of superconductivity at 4.2°K. No magnetic field dependence of the zero-bias resistance was observed at 9.5°K and 20°K for a junction containing particles with an average radius $\sqrt{\langle r^2\rangle}=35$ Å. Since the temperature region 4.2–9.5°K was inaccessible to us for measurements in a high magnetic field we did not experimentally determine the transition temperature in this region.

In Fig. 9 we plot the change in zero-bias resistance as a function of magnetic field for junctions containing different particle sizes. We chose to define the critical

[20] L. Y. L. Shen, Phys. Rev. Letters 21, 361 (1968).

field H^* of a set of particles as the field where the zero-bias resistance has changed by half the total change.

As will be discussed in detail later, the reason for the magnetic field dependence of the zero-bias resistance is that the superconducting energy gap depends upon the magnetic field. For a single particle, H^* is the field where the energy gap becomes comparable to kT and it is, therefore, only approximately equal to the actual critical field when $kT \ll \Delta$. However, as defined, H^* is always smaller than the actual critical field and thus may be regarded as a conservative estimate.

In the experiment we deal with a distribution of particle sizes in a single junction and, therefore, a distribution of critical fields. As long as the resistance decreases as a function of magnetic field we know that at least some of the particles in the junction are still superconducting.

In Fig. 10 we plot the critical field H^* as a function of the inverse average particle radius. The relationship is essentially linear for larger particles but for smaller particles H^* increases very rapidly.

According to Wright,[21] particles with a few hundred angstrom radius are rather flat; however, we expect the smaller particles to be approximately spherical. For particles below 100 Å radius a comparison of the total amount of Sn condensed, as measured by a Sloan crystal-thickness monitor, and the area covered by the particles, as seen in the electron micrographs, suggests that the particles are nearly spherical. A measurement of the critical field H^* as a function of field angle on a set of particles with an average radius $\sqrt{\langle r^2 \rangle} = 80$ Å supports this assumption. H^* is 31 kOe when the magnetic field is applied parallel to the films and 21 kOe when the field is applied perpendicular. Considering the strong radius dependence of H^* in this region, we interpret this result to mean that the particles are nearly spherical.

The critical field H^* at 1°K for particles below $r \sim 60$ Å exceeds the experimentally available field range. For particles with $\sqrt{\langle r^2 \rangle} \sim 30$ Å there is still a slight resistance decrease as a function of field for fields $H > 80$ kOe indicating a H^* of a few hundred kOe (Fig. 11). At 4.2°K there is a more pronounced decrease in resistance as a function of field; thus, we conclude that the particles are definitely superconducting.

Junctions containing particles with $\sqrt{\langle r^2 \rangle} = 18$ Å show only a very weak resistance increase in fields up to 100 kOe at $T = 1$°K and at $T = 3.55$°K. The reason for this background effect is unknown. At 4.2°K a slight resistance decrease for fields above 50 kOe was observed, as shown in Fig. 11. We take this as evidence for superconductivity in at least some of the particles in the junction. The biggest particles in a junction with $\sqrt{\langle r^2 \rangle} = 18$ Å have a radius of about 25 Å. We claim that such particles are superconducting and that they have an energy gap.

[21] F. Wright, Phys. Rev. **163**, 420 (1967).
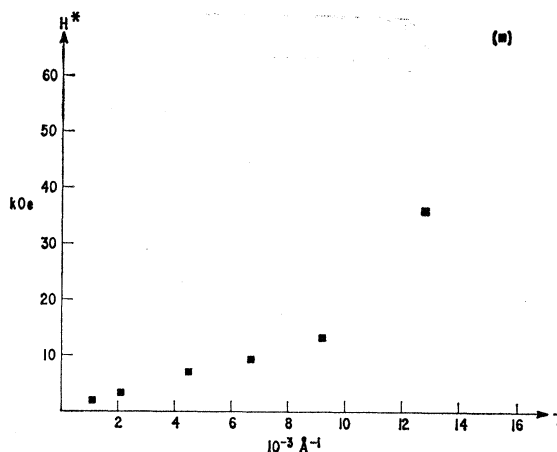

FIG. 10. Critical field H^* at 1°K as a function of inverse average particle radius $1/\sqrt{\langle r^2 \rangle}$. The field is applied parallel to the film. The point in the parentheses corresponds to a conservative estimate of H^* (cf. Fig. 9).

All junctions with smaller particles showed only the weak background resistance change. We can only conclude that they are either normal, have no gap, or that the gap can not be affected by fields up to 100 kOe.

IV. CAPACITOR MODEL OF PARTICLE

A. Particles in Normal State at $T=0$

We shall first develop a model for the case when the Sn particles are in the normal state, and show that our model explains the large temperature-dependent resistance peak observed at zero bias.

It is important to notice that in the radius range considered the spacing of the electron energy levels in a particle is always small compared with the Coulomb energy created by adding or removing one electron from the particle. The work required to charge up a sphere of radius r by the charge of a single electron e is $e^2/2r$, which amounts to about 130 meV for a sphere
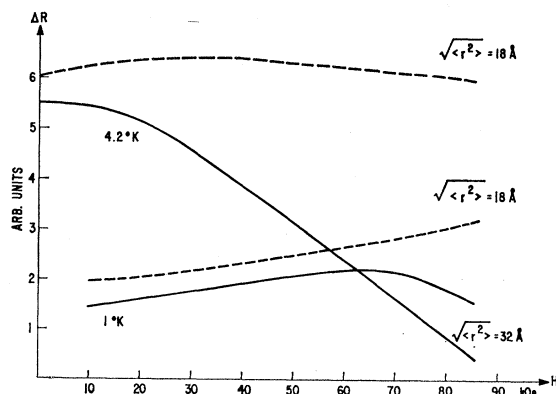

FIG. 11. Magnetic field dependence of the zero-bias resistance at $T=1$°K and $T=4.2$°K for two junctions with average particle radii of 32 Å (solid line) and 18 Å (dashed line). The field direction is parallel to the Al film. One unit in the ordinate corresponds to $\Delta R/R \sim 3\%$.
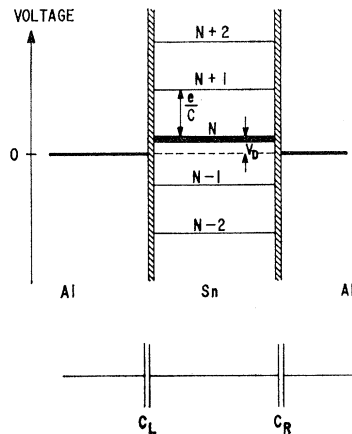
FIG. 12. Schematic illustration of the voltage of a particle as a function of its number of electrons. In equilibrium there are N electrons on the particle. Each change of this number by one changes the voltage of the particle by e/C, where $C=C_L+C_R$ is the capacitance of the particle.

with $r=50$ Å. In our experiment the particles are imbedded in a dielectric matrix. This reduces the above energy by about one order of magnitude. But even so, in explaining the experimental results, the Coulomb energy plays a dominant role. A single particle can, therefore, be treated as a classical capacitor, and as we shall show this model explains all our experimental results. A somewhat similar model has been proposed by Neugebauer and Webb[22] to explain the electrical conductivity along ultrathin metal films.

If contact is made between the two sides of a capacitor which has capacitor plates made of metals with different work functions, electrons are exchanged until the Fermi levels of the two metals are exactly aligned. Despite the fact that there may be a large electric field between the capacitor plates, the capacitor appears now uncharged. A capacitor is uncharged by definition when the Fermi levels of the metals on both sides are aligned. If one of the capacitor plates has a very small physical size, such as our Sn particles, an exact alignment is not possible. The reason for this is that the alignment occurs in discrete voltage steps, $\Delta V=e/C$, where C is the capacitance of the particle. In equilibrium the number of electrons on the particle must be such that it is closest to alignment, but there may still be some voltage difference V_D left. V_D will be restricted by $|V_D|<e/2C$. For particles with $r=50$ Å, ΔV and V_D are of the order of 10 mV. At liquid-helium temperature the number of electrons on such a particle is therefore fixed.

In our case we have small Sn particles in equilibrium with two Al films. The films and any one particle can exchange electrons through tunneling until the equilibrium situation is reached.

When a voltage is applied we get a current flow through the junction. The electrons can flow from one

[22] C. A. Neugebauer and M. B. Webb, J. Appl. Phys. 33, 74 (1962).

side of the junction to the other by essentially three different mechanisms:

(1) direct tunneling through the aluminum oxide, avoiding the Sn particles. This mechanism gives a constant, voltage- and temperature-independent, background conductivity. For properly prepared junctions with a particle radius $r>30$ Å direct tunneling can be made completely negligible even at 1°K and at zero bias.

(2) tunneling from one Al film onto a Sn particle, localizing the electron there and then in turn tunneling out on to the other side. This process needs an activation energy which in turn is responsible for the zero-bias resistance peak. We will discuss this process in most of the remainder of the paper.

(3) tunneling from one aluminum film through a particle and out onto the other aluminum film without actually localizing the electron on the particle. The particle is only involved as an intermediate state; thus, the process is of second order. This process can conceivably become important at low temperatures and at low voltages; however, no experimental evidence has been found for this process. It is very similar in principle to Anderson's model[18] for tunneling involving intermediate magnetic impurity states.

According to process (2), in order to get a current flow the number of electrons on a Sn particle has to be changed by at least one. The activation energy required is equal to the difference of the Coulomb energies in the initial and the final state, i.e.,

$$E=\tfrac{1}{2}(e/C\pm V_D)^2 C-\tfrac{1}{2}V_D^2 C,\qquad(1)$$

where the positive sign holds for adding an electron and the negative sign for subtracting an electron. This activation energy can only be supplied by the battery. We would like to emphasize again that E is a pure classical Coulomb energy, and that all effects due to the level spacing in the particle have been neglected since the level spacing is small compared with E.

The capacitance of a specific particle, C, is simply the sum of the capacitance between the particle and the

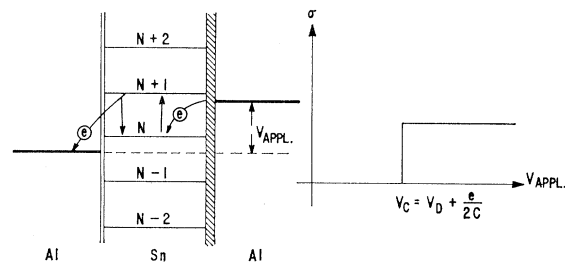FIG. 13. Mechanism of current flow for an asymmetric junction $(C_L\gg C_R)$. An electron from the right film tunnels into the particle, raising its electron number from N to $N+1$ and its voltage from V_D to V_D+e/C. In a next step the electron tunnels out onto the left film bringing the particle back in its ground state. This results in a step function for the conductivity as a function of voltage.

left film C_L and the particle and the right film C_R, as indicated on Fig. 12. When an electron tunnels from the left film into a particle a polarization charge $eC_R/(C_L+C_R)$ will flow from the right film through the battery and into the left film. Thus, the net change in the polarization charge on the left is simply

$$e\frac{eC_R}{C_R+C_L}=e\frac{C_L}{C_R+C_L}=e\frac{C_L}{C}. \tag{2}$$

The work done by the battery must at least equal the activation energy

$$VeC_R/C\geq\tfrac{1}{2}(e/C+V_D)^2C-\tfrac{1}{2}V_D^2C, \tag{3}$$

$$V\geq (C/C_R)(e/2C+V_D), \tag{4}$$

where V is the applied battery voltage. The corresponding condition for an electron tunneling out from a particle onto the film on the right is

$$V\geq (C/C_L)(e/2C-V_D). \tag{5}$$

For current to flow only one of these conditions has to be fulfilled.

In order to calculate the conductivity of a particle as a function of the applied voltage, we consider first the simplest case and assume that the oxide barrier is very asymmetric. Thus, $C\approx C_R\gg C_L$ and the tunneling matrix element between a particle and the right film is much larger than the corresponding one between the particle and the left film. The important consequence of this assumption is that the applied voltage always appears between the particle and the left film. The condition for current flow becomes

$$\begin{matrix} |V|>e/2C+V_D, & \text{for} & V>0 \\ |V|>e/2C-V_D, & \text{for} & V<0 \end{matrix} \tag{6}$$

where $V>0$ is defined such that electrons flow to the right. In ordinary tunneling between normal metals the conductivity $\sigma(V)$ is independent of the applied voltage V for low applied voltages.[23] Using this fact in our case leads to

$$\begin{matrix} \sigma''(V)=0, & \text{for} & -(e/2C-V_D)<V<(e/2C+V_D) \\ \sigma''(V)=\text{const}, & \text{for all other values of } V \end{matrix} \tag{7}$$

where $\sigma''(V)$ is the conductivity of a single particle. Figure 13 shows schematically the conductivity of a single particle as a function of voltage.

The conductivity of a particle is proportional to its area, which is in turn proportional to the capacitance C. We assume that for a set of particles with a given capacitance, V_D is distributed uniformly in the interval $-e/2C<V_D<+e/2C$. The conductivity of a number of particles $f(C)$ with capacitance C is therefore

$$\sigma'(V)\sim Cf(C)\int_0^{e/C} C\theta(|V|-V_c)dV_c, \tag{8}$$

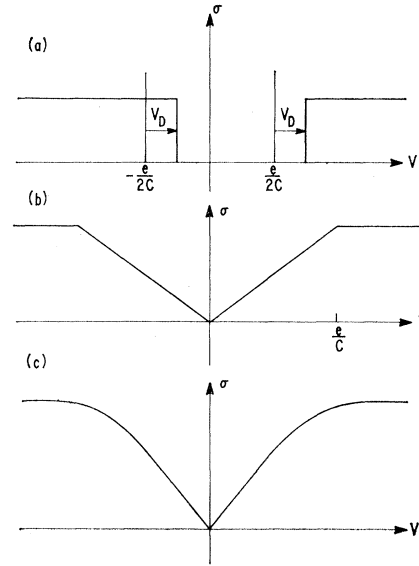[23] J. C. Fisher and I. Giaever, J. Appl. Phys. **32**, 172 (1961).

FIG. 14. Dynamical conductivity as a function of voltage (a) for a single particle, (b) for a set of particles with fixed capacitance C, (c) for a set of particles with a distribution of C.

where $V_c=e/2C+V_D$ and $\theta(V)$ is the unit step function. The conductivity is illustrated in Fig. 14.

In order to get the total conductivity we must sum over all the particles or, what is equivalent over all capacitances,

$$\sigma(V)\sim\int_0^\infty dC\,Cf(C)\int_0^{e/C} C\theta(|V|-V_c)dV_c. \tag{9}$$

This result is based on the assumption of a very asymmetric oxide barrier. In the physically more realistic case of a symmetric oxide barrier but still an asymmetric tunneling matrix element, the calculations get more complicated. In this case the number of electrons on a particle may change by more than one and therefore the mean voltage of a particle will change in steps as a function of applied voltage. However, the final result is very similar to Eq. (9).

$$\sigma(V)\sim\int_0^\infty dC\,Cf(C)\int_0^{2e/C} C\theta(|V|-V_c)dV_c. \tag{10}$$

The only difference is that in the symmetric case the saturation conductivity is reached for $V>2e/C$, while it is reached for $V>e/C$ in the asymmetric case. At first sight this looks obvious because in the symmetric case the voltage drop between one film and the particle is only half the applied voltage at small voltages. But at higher voltages the asymmetry in the tunneling matrix elements keeps the voltage of the particle close to the voltage of the stronger coupled film. This results in a complicated conductivity for a single particle but after averaging over a set of particles the simple formula (10) is obtained.
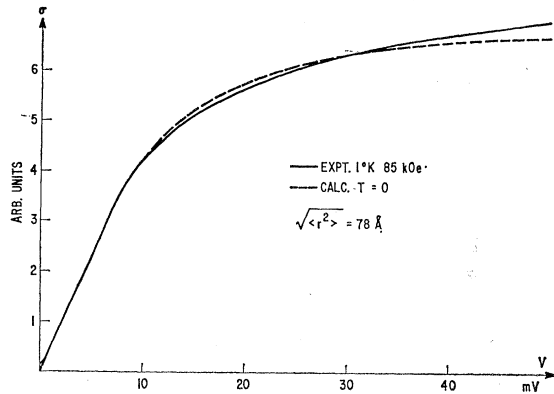
FIG. 15. Measured (solid line) and calculated (dashed line) dynamical conductivity of a set of particles in the normal state. The dashed curve is calculated from the distribution of particle sizes obtained from the electron micrographs using Eq. (10). The only parameter is the proportionality factor between the area of the particle and its capacitance.

In a previous paper[2] we assumed a symmetrical capacitance and symmetrical tunneling matrix elements. The formula given in that paper holds, strictly speaking, only for small voltages because processes like adding or subtracting several electrons from a single Sn particle, which can occur at higher voltages, are not included. For an asymmetric tunneling matrix element we are justified in neglecting these processes because each time an electron flows onto a particle from the weakly coupled film, it is removed to the strongly coupled film before a second electron can flow in. We feel also that the assumption of an asymmetric tunneling matrix element is physically more reasonable because the slightest difference in barrier thickness or barrier height results in a strong asymmetry of the tunneling transition probability. The main result, the existance of a Coulomb activation energy for current flow, does not depend on any of these assumptions.

It is now possible to calculate the conductivity $\sigma(V)$ from the measured particle size distribution using Eq. (10). The only adjustable parameter, except the absolute magnitude of $\sigma(V)$, is the proportionality factor p between the area and the capacitance of the particle:

$$\Delta V = e/C = e/pr^2. \tag{11}$$

In Fig. 15 the dashed curve is calculated from the actual particle size distribution obtained from the electron micrographs. The calculation is independent of the assumption of a symmetric or asymmetric capacitance if we are willing to use p as an adjustable parameter. The best fit is obtained with p corresponding to $\Delta V = 10$ mV for the asymmetric case $(C_R \gg C_L)$ or $\Delta V = 5$ mV for the symmetric case for a particle with 100 Å radius. It should be realized that p is not a purely arbitrary parameter. In principle, p can be calculated from the geometry of the particle in the junction and the dielectric constant of the oxides. A reasonable assump-

tion is to treat the particle as a disklike capacitor assuming a 15-Å-thick oxide layer with a dielectric constant of 10. This results in a calculated $\Delta V = 4$ mV for a $r = 100$ Å particle. We feel that this is in a very satisfactory agreement with the experimental result.

We have determined p for several junctions with different particle sizes. The maximum variation of p never exceeded a factor of 2 and different junctions prepared simultaneously can be described by the same value of p.

B. Particles in the Normal State at $T > 0$

So far we have treated the junction at $T = 0$. At finite temperatures and zero voltage some of the particles have an electron number differing from the equilibrium number because of thermal excitation. By flipping back and forth from the ground state to an excited state these particles are able to carry a current. The zero-bias conductivity $\sigma(0,T)$ is therefore expected to be proportional to the number of excited particles weighted by their area. Considering only one-electron excitations, which is certainly correct for $kT \ll e^2/C$, we get

$$\sigma(0,T) = \int_0^\infty n(V_c)e^{-eV_c/kT}dV_c, \tag{12}$$

where $n(V_c)$ is the area of all particles with activation energy $e^2/2C \pm eV_D = eV_c$. Since V_D is assumed to be uniformly distributed, $n(V_c)$ is constant up to $V_c = e/C$ for particles with a given C. For $kT < e^2/C$ we are therefore allowed to replace $n(V_c)$ by $n(0)$ and take it out of the integral.

$$\sigma(0,T) \sim n(0) \int_0^\infty e^{-eV_c/kT}dV_c \sim T. \tag{13}$$

As can be seen from Fig. 4, this is confirmed very well by the experiment. Since the background conductivity is expected to be temperature-independent in this region, the extrapolated zero-bias conductivity at $T = 0$ gives an estimate of the background conductivity. For not too small particles $(r \gtrsim 30$ Å) the background conductivity is negligible and the total conductivity can be attributed to tunneling via the particles as described above.

C. Particles in the Superconducting State at $T = 0$

The capacitor model is also able to account for the behavior of the junction when the particles are superconducting. As in Sec. III we shall assume that the tunneling matrix element is asymmetric. The current flow is therefore determined by the tunnel probability between the particle and the weaker coupled film.

The main result of the tunneling experiments between a normal and a superconducting metal film is that the

conductivity at $T=0$ is proportional to the super-conducting density of states. In the BCS theory[9] the conductivity is given by

$$\sigma_s{}^{\text{film}}(V) = \frac{|eV|}{[(eV)^2 - \Delta^2]^{1/2}}, \quad |eV| > \Delta$$

$$= 0, \quad |eV| < \Delta$$

where 2Δ is the energy gap of the superconductor. At least in principle our experimental results can be explained by simply taking into account this change in the density of states in the particle when it becomes superconducting. We restrict our discussion to the voltage range $V < 2e/C$. In this voltage range the conductivity of a single particle in the normal state can always be described by a step function no matter what the ratio of the capacitance C_L/C_R is, but at the moment we shall restrict the discussion to the case of an asymmetric junction.

The existence of a Coulomb activation energy implies that we have to replace the constant conductivity in ordinary tunneling between normal metals by a step function $\theta(|V| - V_c)$ to describe the conductivity of a small particle. In analogy with this we must replace the conductivity for tunneling between a normal and a superconducting film $\sigma_s{}^{\text{film}}(V)$ by $\sigma_s{}''(|V| - V_c)$ to describe the conductivity of a single superconducting $\sigma_s{}''(V) = 0$ for $V \le 0$, as shown schematically in Fig. 16. Substituting for the conductivity of a single normal particle $\theta(|V| - V_c)$ by the conductivity of a super-conducting particle $\sigma_s{}''(|V| - V_c)$ in Eq. (9) leads to

$$\sigma_s(V) \sim \int_0^\infty dC\, f(C) C^2 \int_0^{e/C} \sigma_s{}''(|V| - V_c) dV_c, \quad (14)$$

which in the voltage range $|V| < e/C$ can be written as

$$\sigma_s(V) \sim \int_0^\infty dC\, f(C) C^2 \int_0^\infty \sigma_s{}''(|V| - V_c) dV_c,$$

and since $\sigma''(|V| - V_c) = 0$ for $|V| < V_c$,

$$\sigma_s(V) \sim \int_0^{|V|} \sigma_s{}^{\text{film}}(V_c) dV_c. \quad (15)$$

Equation (15) holds for voltages $|V| < e/C$. Note that the conductivity of a particle set is proportional to the integral over the conductivity of a conventional junction between a normal and a superconducting metal film. For small enough particles ($\Delta \gg e/C$) the conductivity-versus-voltage characteristic (Fig. 8) looks qualitatively similar to the current-versus-voltage characteristic of an ordinary tunnel junction.

In the case of an asymmetric tunneling matrix element but an arbitrary capacitance ratio C_L/C_R, only the fraction C_R/C of the applied voltage appears
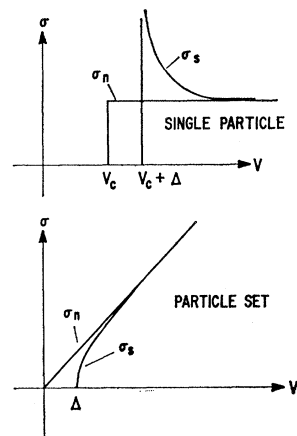

FIG. 16. Voltage dependence of the conductivity in the normal state, σ_n, and in the superconducting state, σ_s, for a single particle and for a set of particles with $e/C \gg \Delta$.

between the particle and the left film (which is assumed to be the weaker coupled). Equation (15) has therefore to be replaced by

$$\sigma_s(V) \sim \int_0^{|V|} \sigma_s{}^{\text{film}}\!\left(\frac{C_R}{C} V_c\right) dV_c.$$

This results in an increased voltage at which the measured step occurs compared to Δ/e and to a smearing of the step given by the distribution of the values of C_R/C in the particle set.

V. DISCUSSION

A. Normal Particles

In order to confirm that the experimental results do not depend at all on the electronic structure of the particles or the films we have done similar experiments on the following systems: Al-Sn particles-Sn, Al-Pb particles-Al, Mg-Sn particles-Mg, Sn-Pb particles-Sn, and Al-Bi particles-Al. All these systems showed a behavior similar to the system Al-Sn particles-Al described above in detail, and the voltage dependence of the conductivity can be explained by our model for the particles both when they are normal or, when applicable, superconducting. This shows that the reason for the zero-bias anomaly in our case is simply due to the capacitor effect which we have described. This model which describes successfully all the experimental facts does not contain a single parameter connected with the electronic structure of the particles or the films except, of course, for superconductivity. Very little physical information can be extracted from the measurements of the zero-bias resistance peak caused by the small particles in the normal state. We have also investigated the properties of Al-Al$_2$O$_3$-Al and Sn-Sn$_x$O$_y$-Sn junctions containing Ti. The junctions have been prepared similarly to the junctions containing Sn particles.

Qualitatively we get the behavior reported by Wyatt and Lythall[11] for Ti-doped junctions prepared in a slightly different way. At Ti concentrations corresponding to several monolayers we observe a giant zero-bias resistance peak. At the rather high Ti concentrations used by us we see no indications of the superimposed zero-bias resistance dip observed in some impurity doped junctions by other authors.[11,12] With the electrodes being superconducting the Ti-doped junction shows qualitatively the same behavior as a junction doped with small metal particles, i.e., no current step at the voltage $2\Delta/e$ but a shift in the current-versus-voltage characteristic similar to Fig. 7. This indicates that the bulk of the current is tunnel current involving real intermediate states. Any scattering processes are relatively unimportant. However, the increase in conductivity as a function of voltage is much stronger than predicted from the small particle model. The intermediate states involved in this process must be of a different nature.

At a pressure of 10^{-6} Torr and the relatively slow evaporation rate used by us, the number of Ti atoms hitting the substrate in a given time is of the same order as the number of impurity atoms. Ti is known to form several oxides, one of which is even metallic. Ti is often used in getter pumps because of its strong tendency to absorb gases; the deposited Ti film is therefore probably very ill defined and is very likely to contain a broad spectrum of localized states with low activation energies.

The capacitor model can easily be generalized by replacing the idea of a small metallic particle by the more general one of a localized impurity state in the barrier. The corresponding process would then be for an electron to tunnel into this state, localize there and in turn tunnel out on the other side. $d\sigma/dV$ at $T=0°K$ gives essentially the distribution of activiation energies in the barrier. Finally, of course, this model merges into the space charge limited conductivity proposed by Shen[21] to explain his results on Pt-doped junctions. When CdS is used as a tunneling barrier the results also indicate that real barrier states are involved in the conduction process. We shall report on this in a separate paper. At the present time the only case where the nature of the barrier states is clear is in the case of our small imbedded particles. It is certainly true that both the so-called giant zero-bias anomaly and some of the smaller zero-bias resistance peaks observed in metal-insulator-metal, metal-Schottky barrier-semiconductor, and p-n semiconductor tunnel junction can be explained by tunneling into real barrier states such as we have discussed here. It seems likely to us, for example, that with the heavy doping necessary to form tunnel junctions in semiconductors clustering of the doping agents might occur, which in turn will act like small imbedded particles, or for that matter real barrier states, and cause resistive peaks at low temperature.

B. Superconducting Particles

De Gennes and Tinkham[24] have calculated the critical field for small superconducting particles. They get that $H_c \sim 1/d^{3/2}$ for the particles if the electron mean free path l is equal to the particle diameter d and $H_c \sim 1/d$ for dirty particles with $l \ll d$. The measured critical field H^* parallel to the film electrodes is plotted in Fig. 10 versus the inverse particle radius. For particles with $r > 100$ Å the critical field is in good approximation proportional to $1/\sqrt{\langle r^2 \rangle}$ but it is much stronger dependent upon size for smaller particles. Since we know that particles with $r > 100$ Å are ellipsoidal rather than spherical a direct comparison with the theory of De Gennes and Tinkham is not quite fair; however, the theory also gives the correct order of magnitude for the critical field for a 100 Å particle if we assume that the particle is spherical. For larger particles the critical field parallel to the film electrodes depends upon the length of the minor axis rather than the length of the visible major axis which is observed in the electron micrographs. To agree with theory if we assume that the electron mean free path is limited by the minor axis, the length of the minor axis must increase as the square root of the observed major axis for particles bigger than $r = 100$ Å. This does not seem unreasonable. However, for particles with $r < 100$ Å the theory of De Gennes and Tinkham cannot account for the observed increase in the critical field.

Di Castro and Valatin[25] have also calculated the superconducting properties of small particles in a high magnetic field. In their theory the action of the field on the electron competes with the pairing interaction. They obtain a $1/r^{5/2}$ dependence of the critical field and H_c is of the order 10^5–10^6 Oe for $r = 25$ Å. This is in qualitative agreement with the experimental results for very small particles ($r < 100$ Å) although the radius dependence of the critical field seems to be even stronger in our experiments.

Even in the case of a very small particle without any Meissner effect there is a theoretical upper limit for the critical field H_c. The condensation energy of a superconductor ΔF has to be larger than the difference in the paramagnetic energy between the normal and the superconducting state.

$$\Delta F > \tfrac{1}{2}(X_n - X_s)H^2,$$

where X_n and X_s is the magnetic susceptibility in the normal and superconducting state. Clogston[26] was the first to propose the so-called paramagnetic limit. Neglecting orbital contributions to the susceptibility, Clogston gets from the simple BCS theory at $T=0°K$

$$H_c^{\max} = 18.4 T_c \text{ kOe } °K^{-1}.$$

In the experiment we see no indication of the para-

[24] P.-G. de Gennes and M. Tinkham, Physics 1, 107 (1964).
[25] C. Di Castro and J. G. Valatin, Phys. Letters 8, 230 (1964).
[26] A. M. Clogston, Phys. Rev. Letters 9, 266 (1962).

magnetic limit as the small particles are superconducting in fields of 100 kOe at 4.2°K, while the above formula would predict $H_c{}^{max} = 68$ kOe at $T = 0°K$. Measurements of the Knight shift of small Sn particles show that the susceptibility in the superconducting state is different from zero, as would be predicted from the simple BCS theory. The ratio of the Knight shifts in the superconducting and the normal state K_s/K_n is of the order of 70% and increases with decreasing particle size. An extrapolation of Wright's[21] results on Sn particles in the radius range 200–400 Å to a radius of 25 Å results in $K_s/K_n \sim 0.9$. The Knight-shift experiments indicate that the actual paramagnetic limit is much higher than predicted by the simple BCS theory. The extrapolation down to particles of 25 Å radius of the Knight-shift data is somewhat dubious for several reasons. Effects like the spacing of the electron energy levels and the difference in the susceptibility of particles having an odd or even number of electrons may become important. Our results, particularly in connection with the increase of T_c, may also indicate an increase in superconducting condensation energy for small particles due to surface effects.[27]

C. Lower Size Limit of Superconductivity

Experimentally we have been able to show that particles with a radius $r = 25$ Å are superconducting and have an energy gap. This is equal to the critical radius predicted by Anderson.[7] While we are able to demonstrate conclusively that bigger particles are superconducting we are not able to prove that smaller particles are always normal.

There can be no doubt, however, that in this size region the bulk theory of superconductivity loses its meaning. As a matter of fact, perhaps we should not even regard the particles as metallic because the energy-level spacing is large compared to kT and because there are very few electrons at the Fermi surface. The

[27] M. Strongin, O. F. Kammerer, J. E. Crow, R. D. Parks, D. H. Douglass, and M. A. Jensen, Phys. Rev. Letters **21**, 1320 (1968).

question of the lower size limit for superconductivity is, therefore, strongly correlated with the definition of superconductivity itself. When we undertook this investigation we expected to find that the transition temperature of a superconductor should be lowered as a function of particle size, and that superconductivity should cease to exist below a certain critical radius. These ideas are not borne out by the experiment. By using a thermodynamical argument it is clear that the transition from the normal to the superconducting state smears out as soon as the total superconducting condensation energy becomes comparable to kT.

Using the bulk critical field of Sn we obtain

$$(H_c{}^2/8\pi)\tfrac{4}{3}\pi r^3 \lesssim kT.$$

For $T \sim T_c$ of Sn this yields a critical radius $r_c \sim 25$ Å. The condensation energy of a single electron is also of the order of kT_c; thus, this thermodynamical argument leads to the same estimate of r_c as Anderson's. At temperatures $T \sim T_c$ thermal fluctuations smear out the superconducting transition for particles where the electron level spacing is of the same order as the energy gap. This means that for $T \ll T_c$ the thermal fluctuations are small compared with the superconducting condensation energy for large particles or with the electron level spacing for small particles. Thus, for $T \ll T_c$ the particle is always in a quantum state which is the superconducting state for large particles and the quantization in momentum space for small particles. While it may be interesting to speculate on what happens in the transition region between the two possible ground states it appears at present not to be especially meaningful experimentally because of the large thermal fluctuations near T_c and the large critical fields required at lower temperatures.
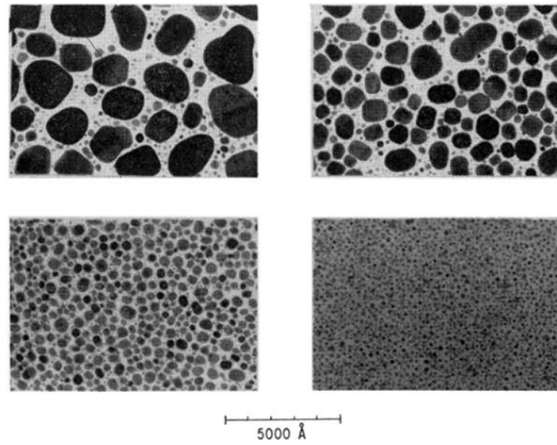
FIG. 2. Electron micrographs of Sn particles on an oxidized
Al film for four different samples.